

Porous organic hydrate crystals: structure and dynamic behaviour of water clusters

Shinji Yamada,*^a Nodoka Sako,^a Kazuhiko Yamada,^b Kenzo Deguchi^c and Tadashi Shimizu^c

^aDepartment of Chemistry, Faculty of Science, Ochanomizu University, Bunkyo-ku Tokyo 112-8610, Japan

^b Research and Education Faculty, in charge of Science Research Center, Kochi University, Oko Campus, Nankoku City, Kochi, 783-8505, Japan.

^cNational Institute for Materials Science and Technology, Tsukuba, Ibaraki 305-0003, Japan

yamada.shinji@ocha.ac.jp

Supporting Information

1. General experimental procedures	S2
2. X-ray structural analysis of 1 ·HCl·3H ₂ O at 123 K	S3
3. Powder X-ray diffraction measurements at 298 K	S13
4. Solid-state [2+2] photodimerization of 1 ·HCl·3H ₂ O and 1 ·HCl	S14
5. ¹³ C and ¹⁷ O NMR measurements and simulations	S15
6. Arrhenius plots	S20
7. TG-DTA measurements of 1 ·HCl·3H ₂ O	S21
8. DSC measurements of 1 ·HCl·3H ₂ O	S22

1. General experimental procedures

X-Ray measurements at 123 K were made on a Rigaku RAXIS RAPID II imaging plate area detector with graphite monochromated Cu-K α radiation. All calculations were performed using the CrystalStructure crystallographic software package except for refinement, which was performed using SHELXL-2013. The raw data frames were integrated with the SAINT+ program by using a narrow-frame integration algorithm. All structures were solved by a combination of direct methods and difference Fourier syntheses, and refined by full-matrix least squares on F₂, by using the SHELXTL software package. Powder X-ray diffraction profiles were recorded using a Rigaku Ultima IV with monochromated Cu-K α radiation ($\lambda = 1.54184$ Å, 50 kV, 40 mA, scan speed 2.0°/min, scan range 4 - 60°) equipped with a cross-beam optics system consisting of a PSA100U parallel slip analyzer. Thermogravimetric analyses were carried out using a TG-DTA2000SA instrument manufactured by Bruker. Three to five milligrams of the crystal samples were heated from 293 K to 448 K in aluminum pans with 5 mm in diameter. A ramping rate of 10 °C/min was used with a nitrogen purge rate of 150 mL/min. DSC measurements were carried out using a Bruker DSC3100SA. In all the experiments the samples were examined in hermetically sealed pans and non hermetically sealed pans under nitrogen atmosphere. UV irradiation was performed using a 250 W high-pressure mercury lamp (ASAHI SPECTRA REX-250). ¹⁷O NMR experiments were carried out at 67.809 MHz on a 11.7 T JEOL ECA 500 spectrometer using a 4 mm magic-angle spinning (MAS) probe at temperatures from 118 to 373 K. Liquid water was used for chemical referencing of ¹⁷O NMR spectra.

2. X-ray structural analysis of 1·HCl·3H₂O at 123 K

Data Collection

A yellow platelet crystal of C₁₃H₁₇ClN₂O₅ having approximate dimensions of 0.300 x 0.070 x 0.050 mm was mounted on a CryoLoop. All measurements were made on a Rigaku R-Axis RAPID diffractometer using graphite monochromated Cu-K α radiation.

The data were collected at a temperature of $-150 \pm 1^\circ\text{C}$ to a maximum 2θ value of 136.5° . A total of 30 oscillation images were collected. A sweep of data was done using ω scans from 80.0 to 260.0° in 30.0° step, at $\chi=54.0^\circ$ and $\phi = 0.0^\circ$. The exposure rate was 60.0 [sec./ $^\circ$]. A second sweep was performed using ω scans from 80.0 to 260.0° in 30.0° step, at $\chi=54.0^\circ$ and $\phi = 90.0^\circ$. The exposure rate was 60.0 [sec./ $^\circ$]. Another sweep was performed using ω scans from 80.0 to 260.0° in 30.0° step, at $\chi = 54.0^\circ$ and $\phi = 180.0^\circ$. The exposure rate was 60.0 [sec./ $^\circ$]. Another sweep was performed using ω scans from 80.0 to 260.0° in 30.0° step, at $\chi = 54.0^\circ$ and $\phi = 270.0^\circ$. The exposure rate was 60.0 [sec./ $^\circ$]. Another sweep was performed using ω scans from 80.0 to 260.0° in 30.0° step, at $\chi = 0.0^\circ$ and $\phi = 0.0^\circ$. The exposure rate was 60.0 [sec./ $^\circ$]. The crystal-to-detector distance was 127.40 mm. Readout was performed in the 0.100 mm pixel mode.

Data Reduction

Of the 15589 reflections were collected, where 2780 were unique ($R_{\text{int}} = 0.0826$); equivalent reflections were merged.

The linear absorption coefficient, μ , for Cu-K α radiation is 23.982 cm^{-1} . An empirical absorption correction was applied which resulted in transmission factors ranging from 0.673 to 0.887. The data were corrected for Lorentz and polarization effects.

Structure Solution and Refinement

The structure was solved by direct methods¹ and expanded using Fourier techniques. The non-hydrogen atoms were refined anisotropically. Hydrogen atoms were refined using the riding model. The final cycle of full-matrix least-squares refinement² on F^2 was based on 2780 observed reflections and 198 variable parameters and converged (largest parameter shift was 0.00 times its esd) with unweighted and weighted agreement factors of:

$$R1 = \Sigma ||F_o| - |F_c|| / \Sigma |F_o| = 0.0911$$

$$wR2 = [\Sigma (\omega (F_o^2 - F_c^2)^2) / \Sigma \omega(F_o^2)^2]^{1/2} = 0.2706$$

The goodness of fit³ was 1.21. Unit weights were used. Plots of $\sum \omega (|F_o| - |F_c|)^2$ versus $|F_o|$, reflection order in data collection, $\sin \theta/\lambda$ and various classes of indices showed no unusual trends. The maximum and minimum peaks on the final difference Fourier map corresponded to 0.86 and -0.27 e⁻/Å³, respectively. The final Flack parameter⁴ was 0.40(3), indicating that the structure is inversion-twin.⁵

Neutral atom scattering factors were taken from International Tables for Crystallography (IT), Vol. C, Table 6.1.1.4⁶. Anomalous dispersion effects were included in F_{calc} ⁷; the values for $\Delta\phi'$ and $\Delta\phi''$ were those of Creagh and McAuley⁸. The values for the mass attenuation coefficients are those of Creagh and Hubbell⁹. All calculations were performed using the CrystalStructure¹⁰ crystallographic software package except for refinement, which was performed using SHELXL2013¹¹. Crystal data, data collection parameters, and results of the analyses are listed in Tables S1-S3.

References

(1) SHELXS2013: Sheldrick, G. M. (2008). Acta Cryst. A64, 112-122.

(2) Least Squares function minimized: (SHELXL2013)

$$\sum w(F_o^2 - F_c^2)^2 \quad \text{where } w = \text{Least Squares weights.}$$

(3) Goodness of fit is defined as:

$$[\sum w(F_o^2 - F_c^2)^2 / (N_o - N_v)]^{1/2}$$

where: N_o = number of observations

N_v = number of variables

(4) Parsons, S. and Flack, H. (2004), Acta Cryst. A60, s61.

(5) Flack, H.D. and Bernardinelli (2000), J. Appl. Cryst. 33, 114-1148.

(6) International Tables for Crystallography, Vol.C (1992). Ed. A.J.C. Wilson, Kluwer Academic Publishers, Dordrecht, Netherlands, Table 6.1.1.4, pp. 572.

(7) Ibers, J. A. & Hamilton, W. C.; Acta Crystallogr., 17, 781 (1964).

(8) Creagh, D. C. & McAuley, W.J. ; "International Tables for Crystallography", Vol C, (A.J.C. Wilson, ed.), Kluwer Academic Publishers, Boston, Table 4.2.6.8, pages 219-222 (1992).

(9) Creagh, D. C. & Hubbell, J.H.; "International Tables for Crystallography", Vol C, (A.J.C. Wilson, ed.), Kluwer Academic Publishers, Boston, Table 4.2.4.3, pages 200-206 (1992).

(10) CrystalStructure 4.1: Crystal Structure Analysis Package, Rigaku Corporation (2000-2014). Tokyo 196-8666, Japan.

(11) SHELXL2013: Sheldrick, G. M. (2008). Acta Cryst. A64, 112-122.

Table S1. Crystal Data

Empirical Formula	C ₁₃ H ₁₇ ClN ₂ O ₅
Formula Weight	316.74
Crystal Color, Habit	yellow, platelet
Crystal Dimensions	0.300 X 0.070 X 0.050 mm
Crystal System	orthorhombic
Lattice Type	Primitive
Lattice Parameters	a = 6.7596(4) Å b = 14.2927(6) Å c = 16.0445(7) Å V = 1550.11(12) Å ³
Space Group	P2 ₁ 2 ₁ 2 ₁ (#19)
Z value	4
D _{calc}	1.357 g/cm ³
F ₀₀₀	664.00
μ(CuKα)	23.982 cm ⁻¹

Table S2. Intensity Measurements

Diffractometer	R-AXIS RAPID
Radiation	CuK α (λ = 1.54187 Å) graphite monochromated
Voltage, Current	50kV, 100mA
Temperature	-150.0°C
Detector Aperture	460 x 256 mm
Data Images	30 exposures
w oscillation Range (χ =54.0, ϕ =0.0)	80.0 - 260.0°
Exposure Rate	60.0 sec./°
w oscillation Range (χ =54.0, ϕ =90.0)	80.0 - 260.0°
Exposure Rate	60.0 sec./°
w oscillation Range (χ =54.0, ϕ =180.0)	80.0 - 260.0°
Exposure Rate	60.0 sec./°
w oscillation Range (χ =54.0, ϕ =270.0)	80.0 - 260.0°
Exposure Rate	60.0 sec./°
w oscillation Range (χ =0.0, ϕ =0.0)	80.0 - 260.0°
Exposure Rate	60.0 sec./°
Detector Position	127.40 mm
Pixel Size	0.100 mm
$2\theta_{\max}$	136.5°
No. of Reflections Measured	Total: 15589 Unique: 2780 (R_{int} = 0.0826) Parsons quotients (Flack x parameter): 431
Corrections	Lorentz-polarization Absorption (trans. factors: 0.673 - 0.887)

Table S3. Structure Solution and Refinement

Structure Solution	Direct Methods (SHELXS2013)
Refinement	Full-matrix least-squares on F^2
Function Minimized	$\Sigma w (F_o^2 - F_c^2)^2$
Least Squares Weights	$w = 1 / [\sigma^2(F_o^2) + (0.1557 \cdot P)^2 + 0.0000 \cdot P]$ where $P = (\text{Max}(F_o^2, 0) + 2F_c^2)/3$
$2\theta_{\text{max}}$ cutoff	136.5°
Anomalous Dispersion	All non-hydrogen atoms
No. Observations (All reflections)	2780
No. Variables	198
Reflection/Parameter Ratio	14.04
Residuals: R1 ($I > 2.00\sigma(I)$)	0.0911
Residuals: R (All reflections)	0.1260
Residuals: wR2 (All reflections)	0.2706
Goodness of Fit Indicator	1.036
Flack Parameter	0.40(3)
Max Shift/Error in Final Cycle	0.000
Maximum peak in Final Diff. Map	0.89 e ⁻ /Å ³
Minimum peak in Final Diff. Map	-0.28 e ⁻ /Å ³

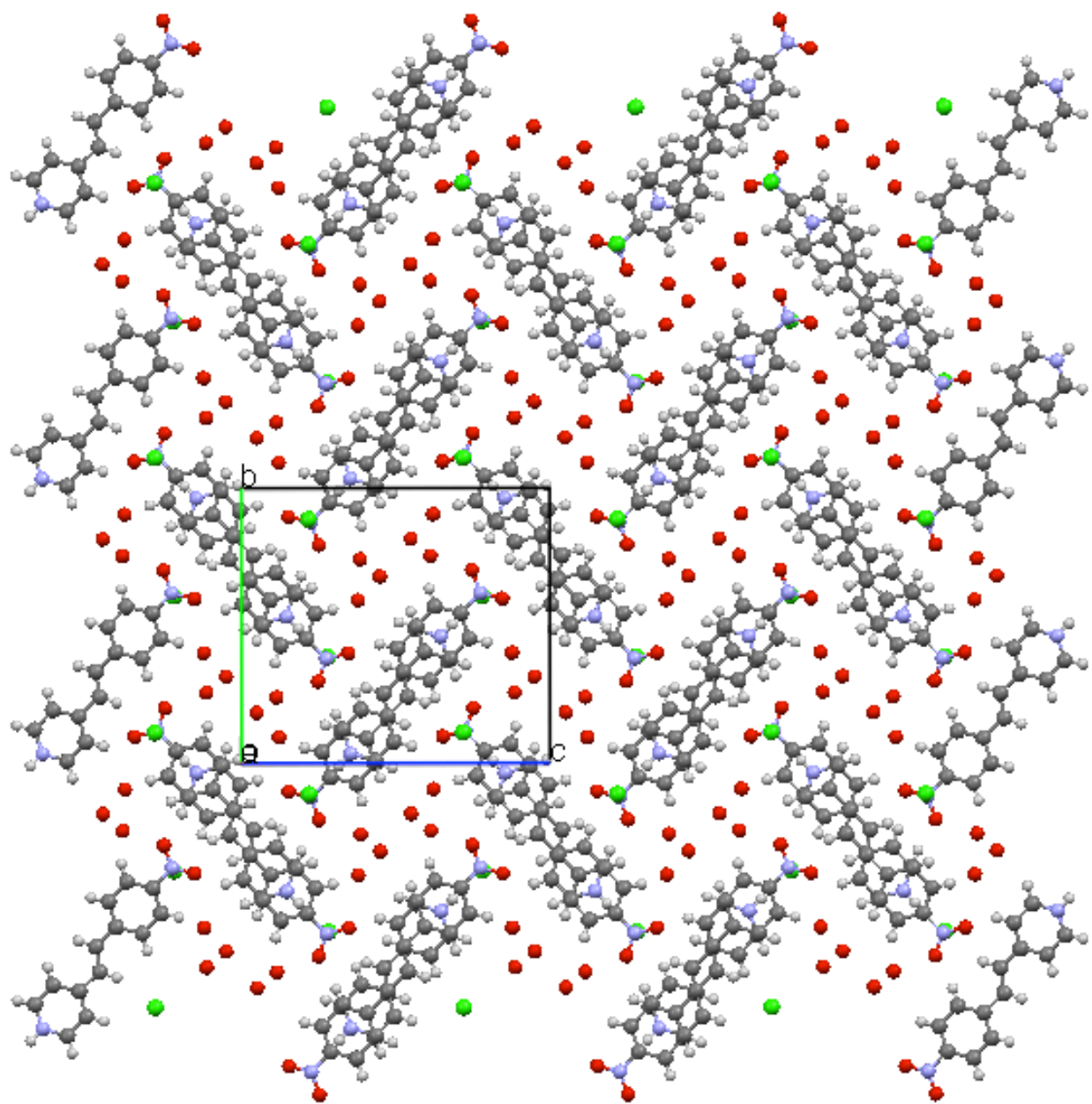


Fig. S1. Packing diagram of 1·HCl·3H₂O down the *a* axis.

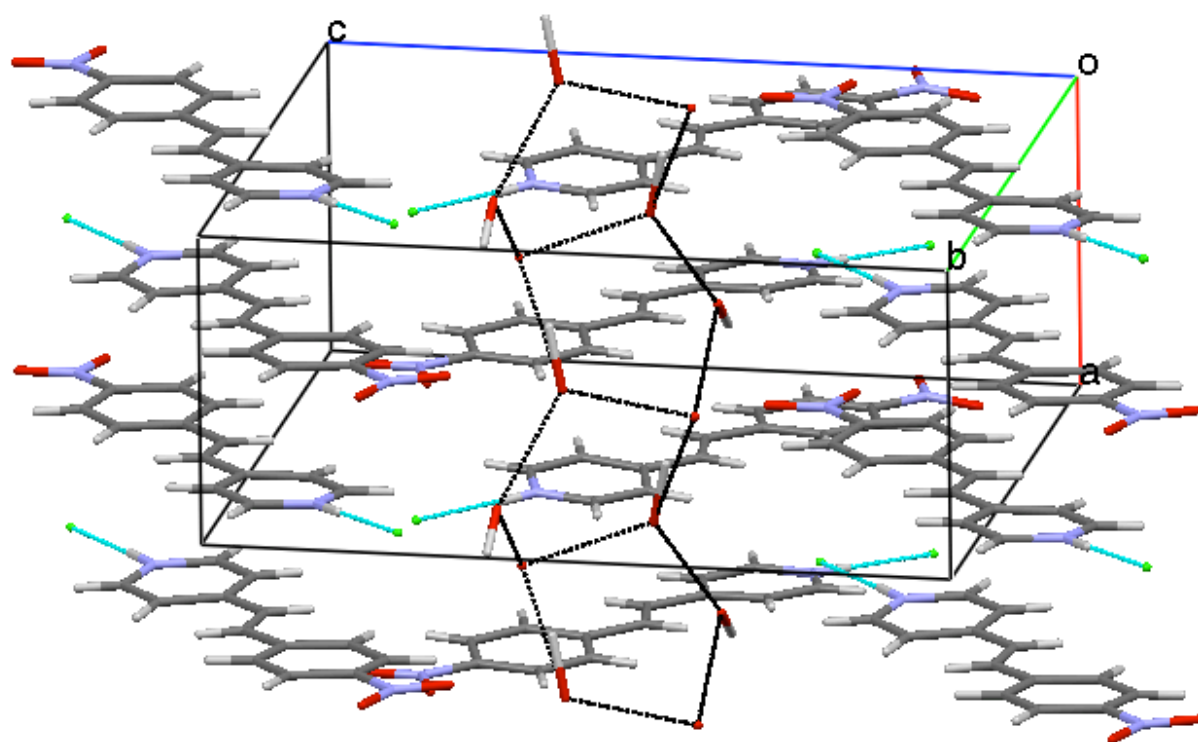


Fig. S2. X-ray structure of the water cluster with the surrounded columns

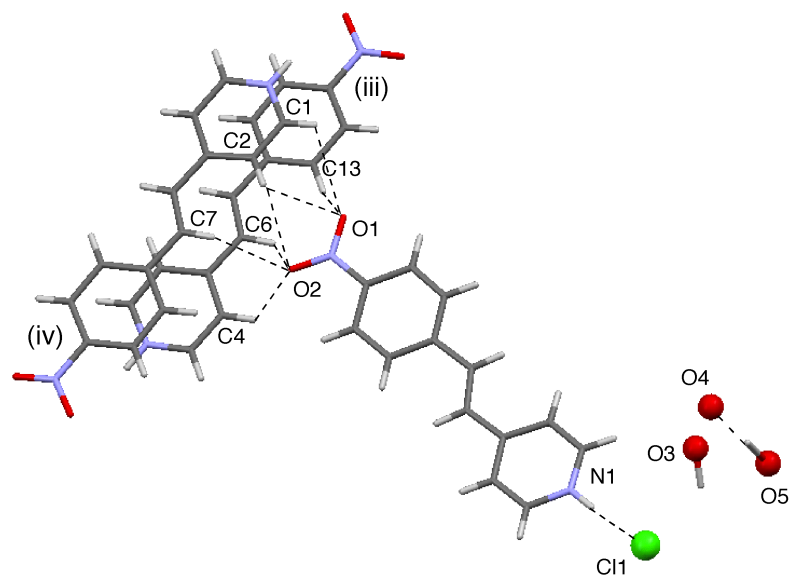


Fig. S3. Intermolecular hydrogen bonds: (iii) $-X+2, Y-1/2, -Z+1/2$; (iv) $-X+3/2, -Y+1, Z+1/2$.

Table S4. Distances of intermolecular hydrogen bonds in the crystal $1 \cdot \text{HCl} \cdot 3\text{H}_2\text{O}$.

Donor	H	Acceptor	D...A	D-H	H...A	D-H...A
N1	H1	Cl1	3.020(7)	0.88	2.14	177
C2 ⁴	H2 ⁴	O1	3.178(9)	0.95	2.72	110
C2 ⁴	H2 ⁴	O2	3.421(9)	0.95	2.68	135
C4 ³	H4 ³	O2	3.193(10)	0.95	2.61	120
C7 ⁴	H7 ⁴	O2	3.406(9)	0.95	2.62	141
C1 ⁴	H1A ⁴	O1	3.256(9)	0.95	2.86	106
C13 ³	H13 ³	O1	3.345(9)	0.95	2.57	138
C6 ³	H6 ³	O2	3.316(9)	0.95	2.72	121
O5	H3	O4	2.938(13)	1.35(6)	1.67(6)	154(4)

^a Symmetry transformations used to generate equivalent atoms: (3) $-X+2, Y-1/2, -Z+1/2$; (4) $-X+3/2, -Y+1, Z+1/2$.

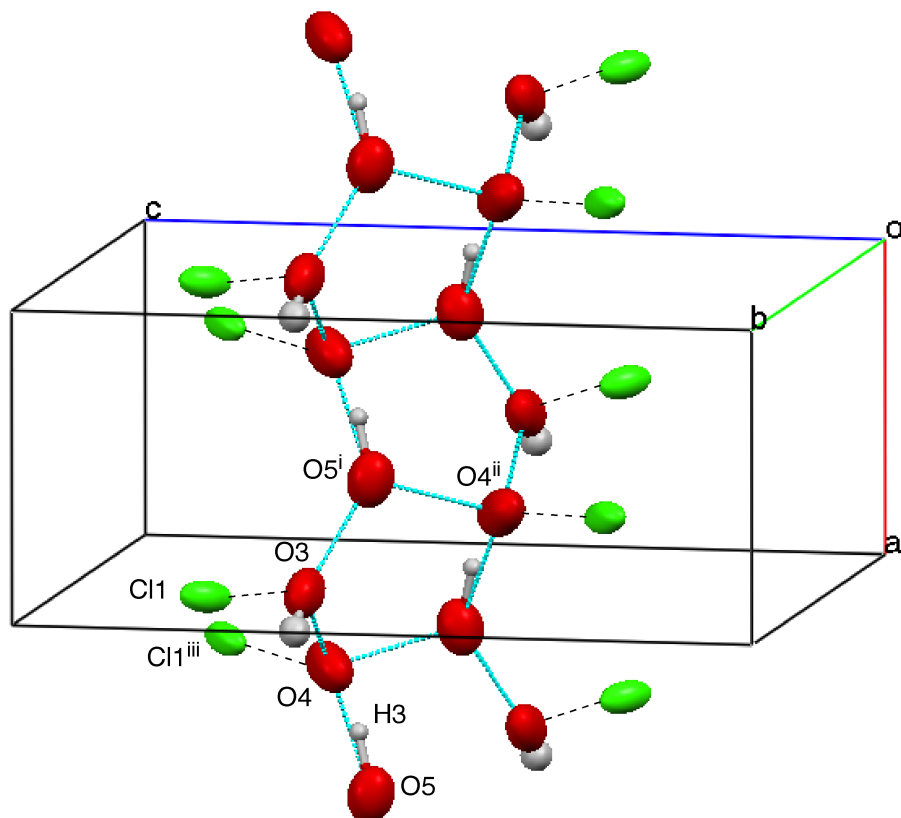


Fig. S4. X-ray structure of the water cluster of $1 \cdot \text{HCl} \cdot 3\text{H}_2\text{O}$. (i) $X-1, Y, Z$; (ii) $X+1/2, -Y+3/2, -Z+1$; (iii) $-X+2, Y-1/2, -Z+3/2$.

Table S5. Distances of intermolecular distances in the water cluster of $1 \cdot \text{HCl} \cdot 3\text{H}_2\text{O}$.

O...X	distance / Å
O3...O4	2.791(13)
O3...O5 ⁱ	2.866(13)
O4...O5	2.938(13)
O5...O4 ⁱⁱ	2.926(11)
O3...Cl1	3.371(10)
O4...Cl1 ⁱⁱ	3.397(9)
O4...H3-O5	1.67(6)

^a Symmetry transformations used to generate equivalent atoms:

(i) $X-1, Y, Z$; (ii) $X+1/2, -Y+3/2, -Z+1$; (iii) $-X+2, Y-1/2, -Z+3/2$.

3. Powder X-ray diffraction measurements of $1 \cdot \text{HCl}$ at 298 K

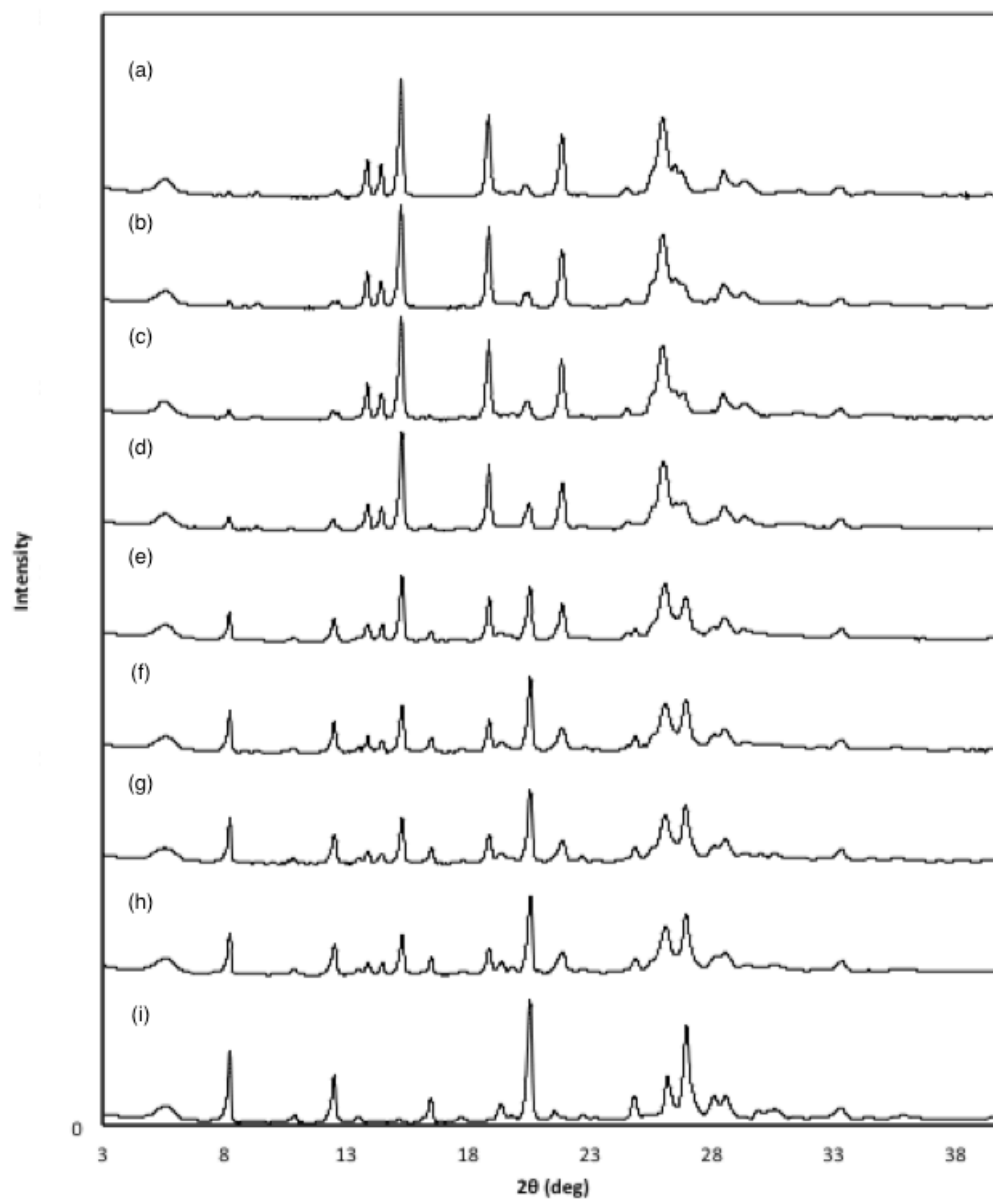


Fig. S5. Time dependence of X-ray diffraction measurements of $1 \cdot \text{HCl}$ under the atmosphere of water vapor at 298 K. (a) before exposure to water vapor, (b) rehydration for 0.5h, (c) 1h, (d) 2.5h, (e) 4h, (f) 5.5h, (g) 7h, (h) 8.5h, (i) 24h, the pattern was in agreement with that of $1 \cdot \text{HCl} \cdot 3\text{H}_2\text{O}$

4. Solid-state [2+2] photodimerization of **1**·HCl·3H₂O and **1**·HCl

The powdered crystals of **1**·HCl·3H₂O (5.1 mg) placed between two Pyrex plates were irradiated with 250W high-pressure mercury lamp for 6h. The crude product was collected and was neutralized with saturated NaHCO₃ solution. This was extracted with CH₂Cl₂ and dried over anhydrous MgSO₄. Evaporation of the organic solvent gave only *syn*HT dimer **2**, the structure of which was confirmed by comparison with the ¹H NMR spectra with those reported. Similarly, the powdered crystals of **1**·HCl (5.3 mg) were irradiated for 16h and *syn*HT dimer **2** was obtained in >99% yield. This suggests that the orientation of molecules are retained after dehydration.

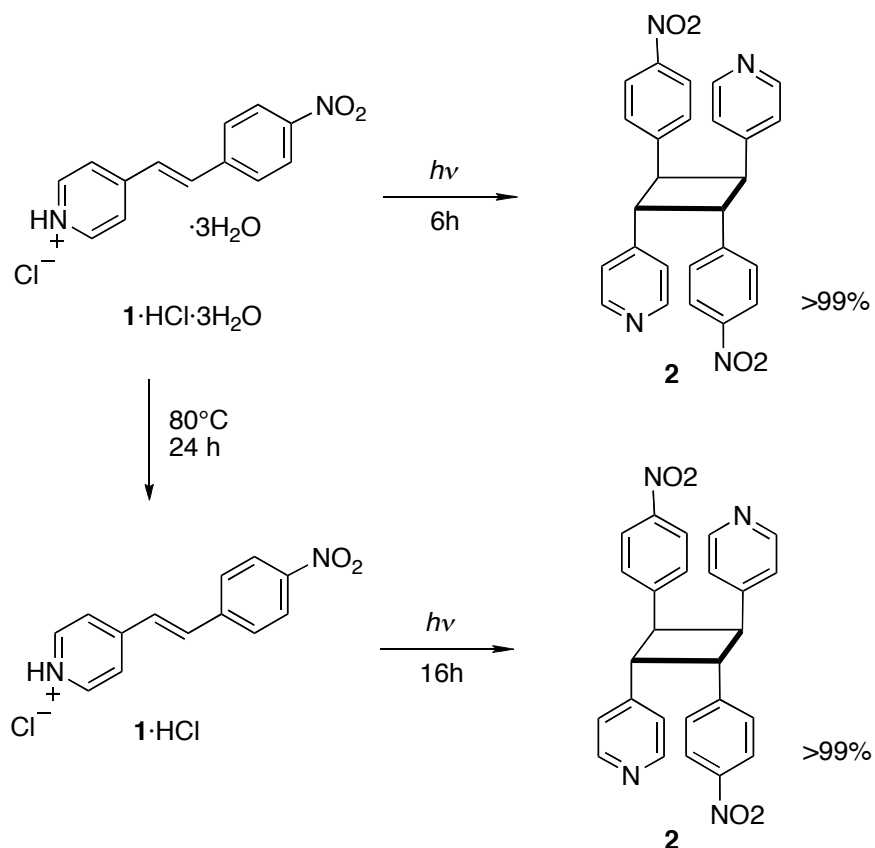


Fig. S6. Solid-state irradiation of **1**·HCl·3H₂O and **1**·HCl

5. ^{13}C and ^{17}O NMR measurements and spectral simulations

NMR measurements

NMR measurements: ^{13}C and ^{17}O NMR experiments were carried out at 125.774 and 67.809 MHz, respectively, on a 11.7 T JEOL ECA 500 spectrometer using a 4 mm magic-angle spinning (MAS) probe at temperatures from 118 to 373 K. Potassium bromide was used for magic-angle adjustment, and adamantane and liquid water were used for chemical referencing of ^{13}C and ^{17}O NMR spectra, respectively. For ^{13}C cross-polarization (CP) MAS experiments, a standard ramped CP sequence was used with the mixing time of 0.5–5 ms and with high-power irradiation or two-pulse phase modulations [ref] for heteronuclear decoupling during the detection periods. The MAS frequencies were set to $10,000 \pm 3$ Hz. The recycle delay time and number of accumulation were typically 5–60 s and 100–200, respectively. For ^{17}O NMR experiments, a quadrupole echo proposed by Kunwar et al. [ref] was used with high-power irradiation for ^1H decoupling during the detection periods. The ^{17}O $\pi/2$ pulse width was 1.7 μs and accumulations of 100–200 were sufficient for most of the ^{17}O NMR spectra. All the NMR spectra were processed by Delta software (JEOL USA Inc.).

Spectral simulations

All the spectral simulations for line-shape analysis of ^{17}O stationary NMR spectra were performed using the program written by the authors on MATLAB (The Math-Works, Inc). There are a few different models in the literature concerning the analysis of water molecular reorientations by solid-state NMR studies.² We believe that the theoretical model proposed by Ratcliffe and co-workers³ is the most effective procedure. Thus, we follow their procedure in the present study. In this model, twelve orientations and four-step jumps of a water molecule are considered for the water molecular reorientation. There are several assumptions in this model: (1) the two hydrogen atoms are distinguished each other, (2) the coordination of a water molecule is tetrahedral, (3) a single rotation is involved in O–H bond only, (4) the exchange rate, τ , is equivalent for all the site-jumps. The semiclassical Bloch-McConnell formalism for chemical exchange⁴ was used to simulate the line-shapes of ^{17}O stationary NMR spectra of water molecules in $1\cdot\text{HCl}\cdot 3\text{H}_2\text{O}$. The details are well described in the literature by R. W. Schurko et al.⁵.

In the present work, only second-order quadrupolar interactions are considered for the spectral simulation because the span of the ^{17}O chemical shielding tensor, defined by $\delta_{11}-\delta_{33}$, was previously calculated to be approximately 40 ppm⁶, while the spectral width involved with the second-order quadrupole interactions at 11.7 T is estimated to be more than 700 ppm.

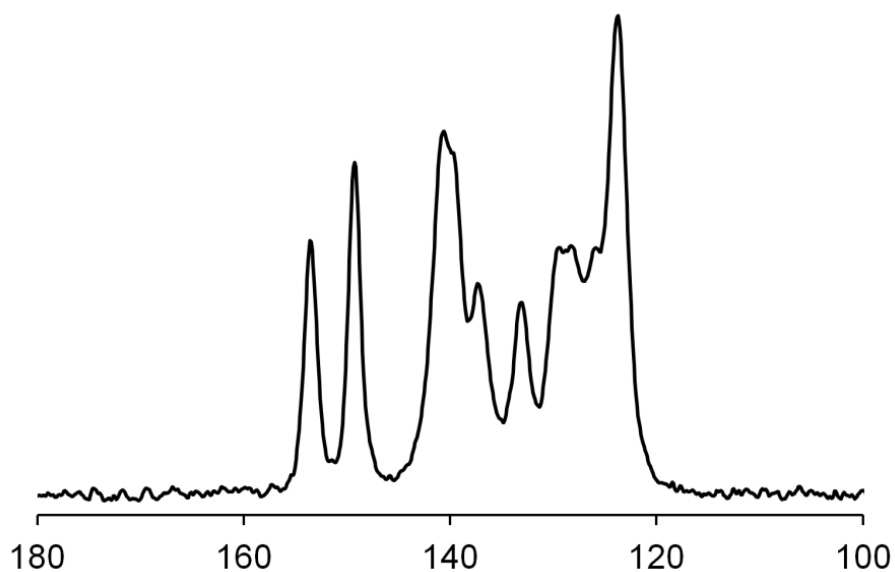
Fig. S9 shows (left) experimental and (right) best-fitted calculated ^{17}O stationary NMR spectra of $\mathbf{1}\cdot\text{HCl}\cdot 3\text{H}_2\text{O}$ at several temperatures. The observed temperatures and rate constants used for the theoretical line-shapes, τ , are given at each spectrum. In the spectral simulation, the literature values of $C_Q = 6.66$ MHz and $\eta_Q = 0.935$ [S6-7] were used with the assumption that the three crystallographically different oxygen sites are equivalent since a static NMR spectrum without molecular motions could not be observed.

References

- (1) Kunwar, A.C.; Turner, G. L.; Oldfield, E. *J. Magn. Reson.* **1986**, *69* 124-127.
- (2) (a) Wittebort, R. J.; Usha, M. G.; Ruben, D. J.; Wemmer, D. E.; Pines, A. *J. Am. Chem. Soc.* **1988**, *110*, 5668-5671. (b) Spiess, H. W.; Sillescu, H. *J. Magn. Reson.* **1981**, *42*, 381-389. (c) Wittebort, R. J.; Olejniczak, E. T.; Griffin, R. G. *J. Chem. Phys.* **1987**, *86*, 5411-5420.
- (3) Same as #16 in the text.
- (4) Same as #17 in the text.
- (5) Schurko, R. W.; Wi, S.; Frydman, L. *J. Phys. Chem. A* **2002**, *106*, 51-62.
- (6) Pennanen, T. S.; Vaara, J.; Lantto, P.; Sillanpaa, A. J.; Laasonen, K.; Jokisaari, J. *J. Am. Chem. Soc.* **2004**, *126*, 11093-11102.
- (7) Spiess, H. W.; Garrett, B.B.; Sheline, R. K. *J. Chem. Phys.* **1969**, *51*, 1201-1205.

^{13}C CPMAS NMR spectra of hydrate $1\cdot\text{HCl}\cdot 3\text{H}_2\text{O}$ and dehydrate $1\cdot\text{HCl}$

(a)



(b)

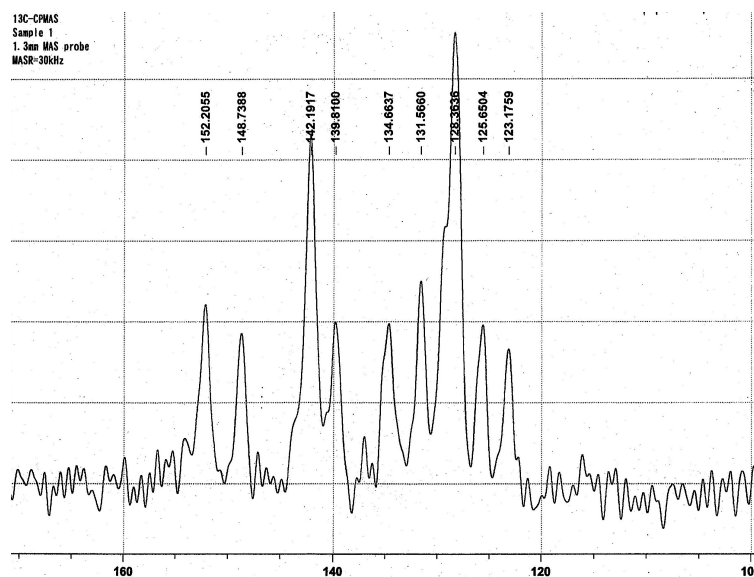


Fig. S7. ^{13}C CPMAS NMR spectra of (a) $1\cdot\text{HCl}\cdot 3\text{H}_2\text{O}$ and (b) dehydrate $1\cdot\text{HCl}$ at 298 K, acquired at 11.7 T with the sample MAS frequency of 10 kHz.

^{13}C CPMAS NMR spectra of hydrate $1\cdot\text{HCl}\cdot 3\text{H}_2\text{O}$ in a sealed sample holder

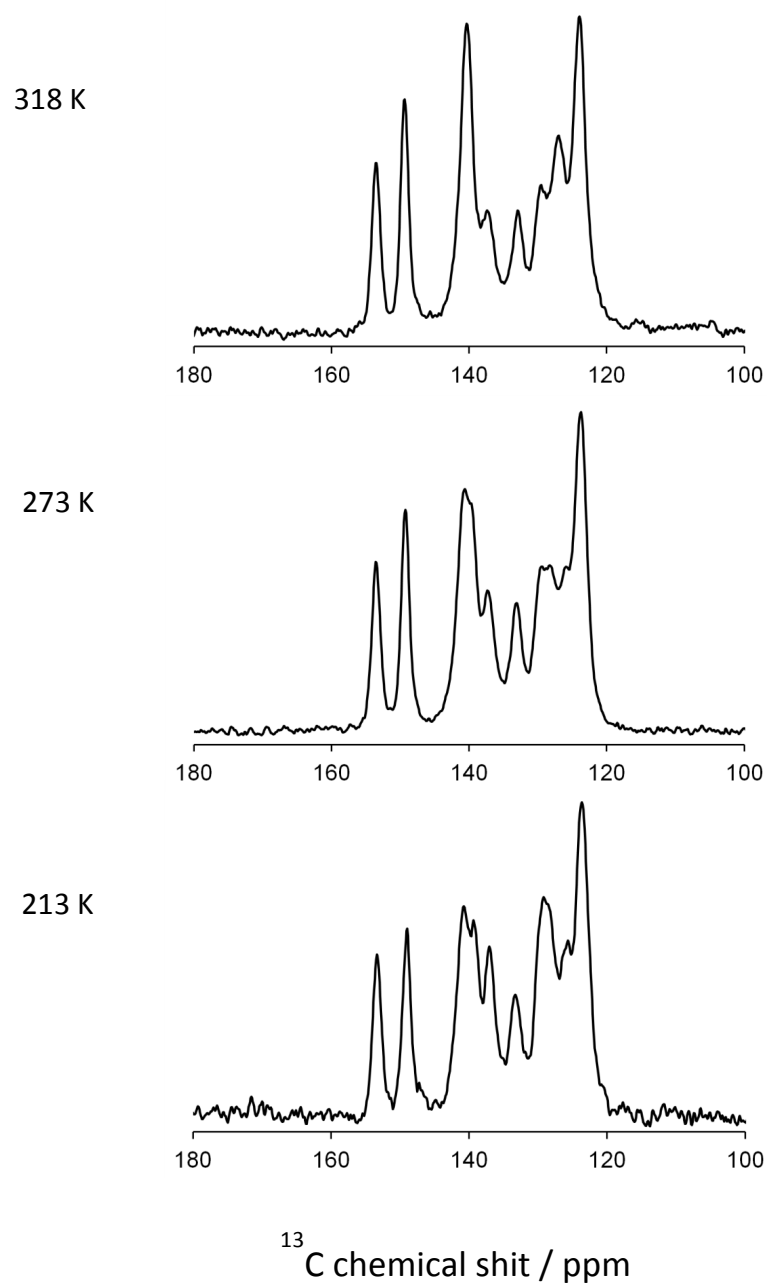


Fig. S8. ^{13}C CPMAS NMR spectra of $1\cdot\text{HCl}\cdot 3\text{H}_2\text{O}$ as a function of temperature, acquired at 11.7 T with the sample MAS frequency of 10 kHz.

^{17}O stationary NMR spectra

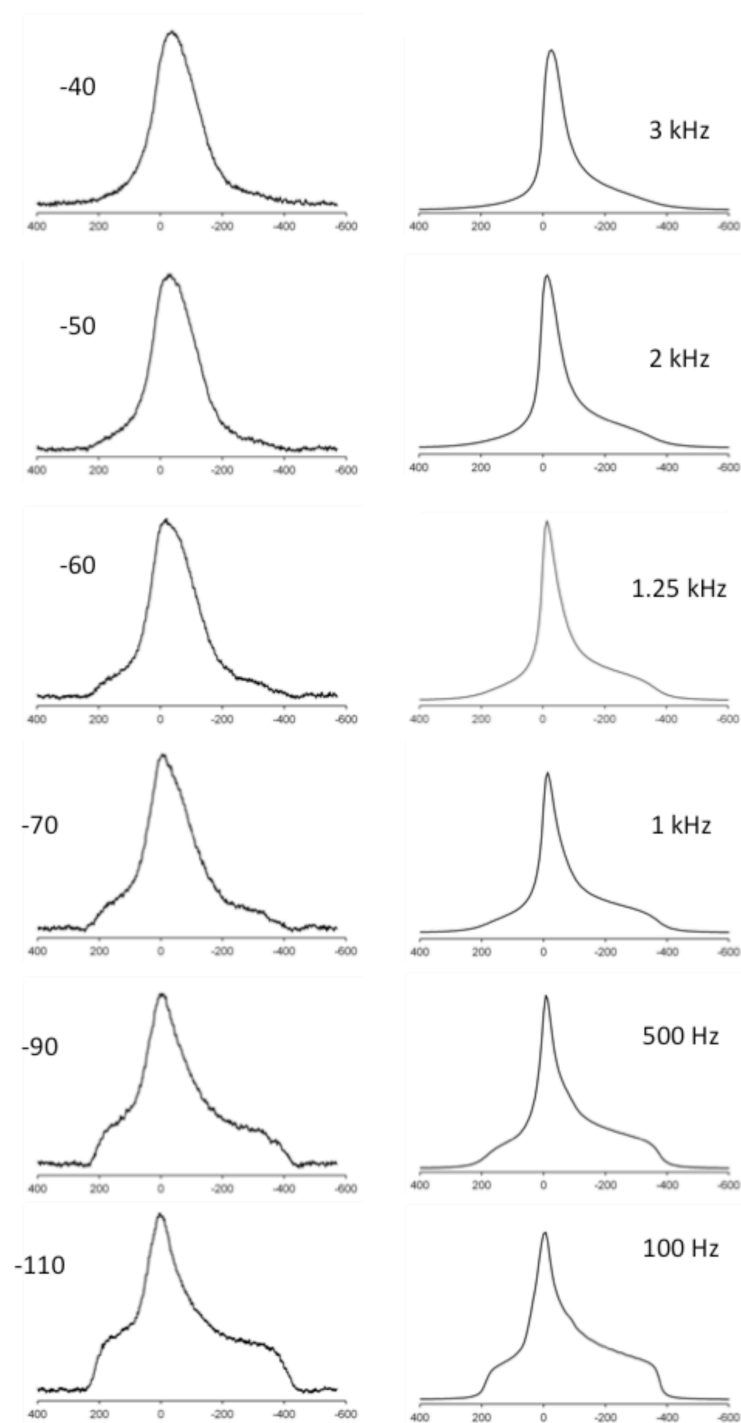


Fig. S9. (left) Experimental and (right) best-fitted calculated ^{17}O stationary NMR spectra of $1\cdot\text{HCl}\cdot 3\text{H}_2\text{O}$ at several temperatures. The observed temperatures and rate constants used for the theoretical line-shapes, t , are given at each spectrum.

6. Arrhenius plots

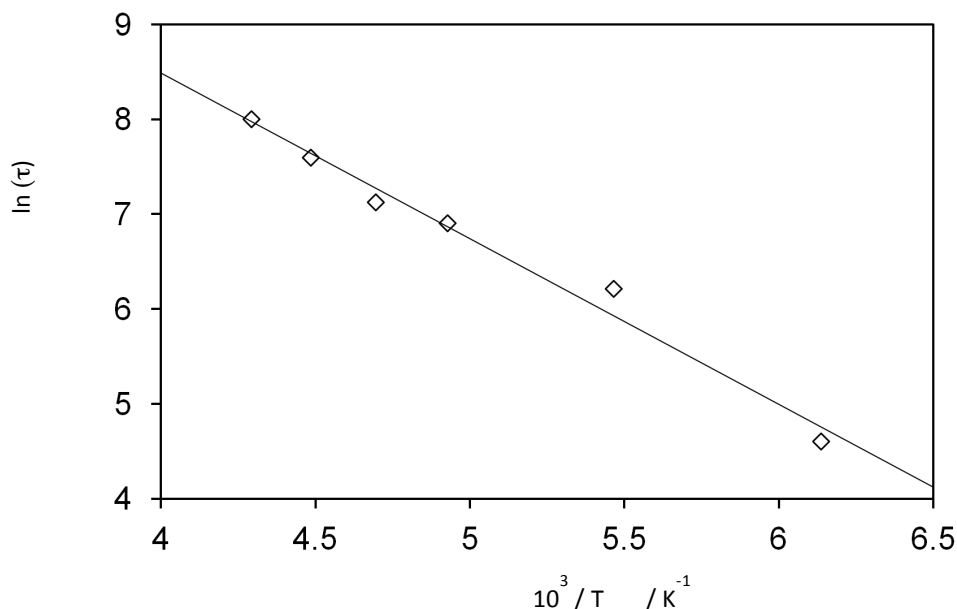


Fig. S10. A plot of $\ln(t)$ versus $10^3/T$ for $\mathbf{1} \cdot \text{HCl} \cdot 3\text{H}_2\text{O}$, together with the least-square liner fit.

With the exchange rate at each temperature, activation energy can be determined by using the Arrhenius law,

$$\tau = L \cdot \exp\left(-\frac{E_a}{RT}\right)$$

where E_a , R , and L are the activation energy in J mol^{-1} , the gas constant of $8.314 \text{ JK}^{-1}\text{mol}^{-1}$, and a constant, respectively. As shown in Figure S9, the least-square fitting to the experimental data provided the activation energy of $E_a = 15 \pm 5 \text{ kJ mol}^{-1}$. As expected, the present result is much smaller than those previously reported for ice and the related molecules ($E_a = 30.12\text{--}59.8 \text{ kJ mol}^{-1}$), indicating that the water molecular reorientations are much more easily carried out in $\mathbf{1} \cdot \text{HCl} \cdot 3\text{H}_2\text{O}$. This is because intermolecular interactions between water molecules and the host compound are weak.

7. DTA measurements of $1 \cdot \text{HCl} \cdot 3\text{H}_2\text{O}$

For compound $1 \cdot \text{HCl} \cdot 3\text{H}_2\text{O}$, TG-DTA experiments in the temperature interval 293 K – 448 K were carried out at a heating rate of 5 K/min. A peak over the temperature range 293 K – 320 K ($T_{\text{peak}} = 312.4 \text{ K}$) was observed in DTA measurement with a 10.89 wt% loss, which is corresponding to a loss of three water molecules.

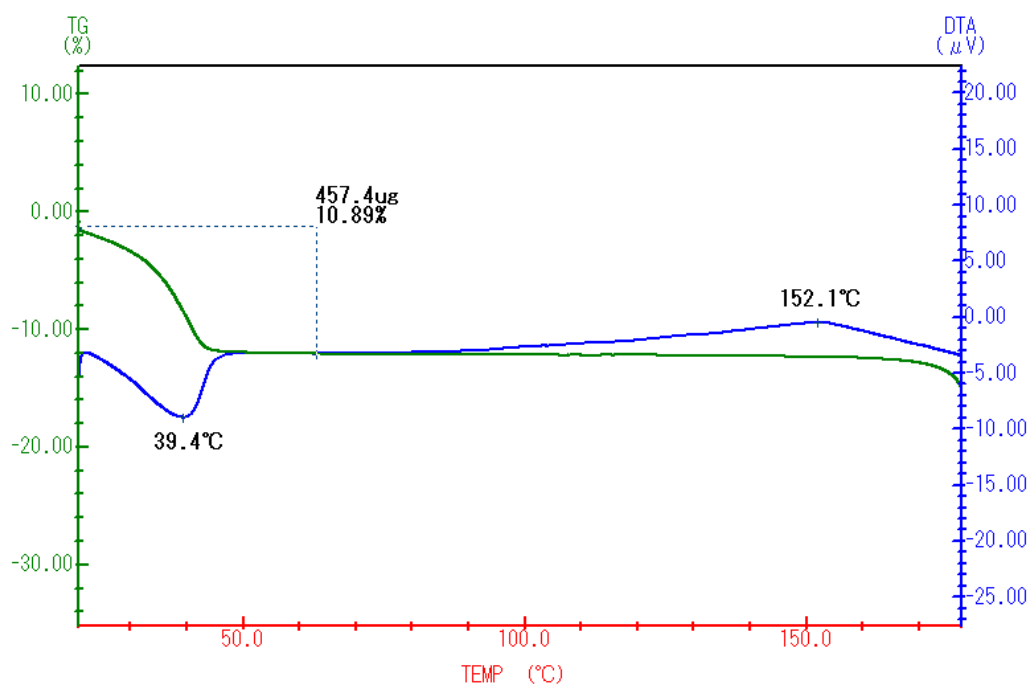


Fig. S11. TG-DTA data for $1 \cdot \text{HCl} \cdot 3\text{H}_2\text{O}$

8. DSC measurements of $1 \cdot \text{HCl} \cdot 3\text{H}_2\text{O}$

For compound $1 \cdot \text{HCl} \cdot 3\text{H}_2\text{O}$, differential scanning calorimetry (DSC) experiments were carried out. The sample was equilibrated inside the calorimeter at $T = 298 \text{ K}$ and then heated at a rate of 5 K/min until 423 K . The measurements were carried out in hermetically sealed pans and non hermetically sealed pans, which were shown in Figure S12 and S13, respectively.

DSC measurement of $1 \cdot \text{HCl} \cdot 3\text{H}_2\text{O}$ in a hermetically sealed pan

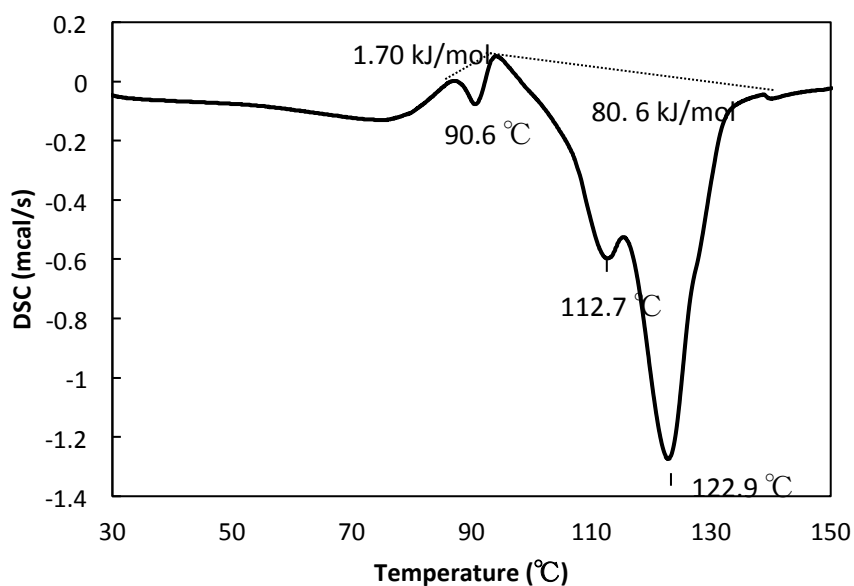


Fig. S12. DSC thermogram of $1 \cdot \text{HCl} \cdot 3\text{H}_2\text{O}$ showing the water molecules remain in the channel by 363 K .

DSC measurement of $1\cdot\text{HCl}\cdot 3\text{H}_2\text{O}$ in a non hermetically sealed pan

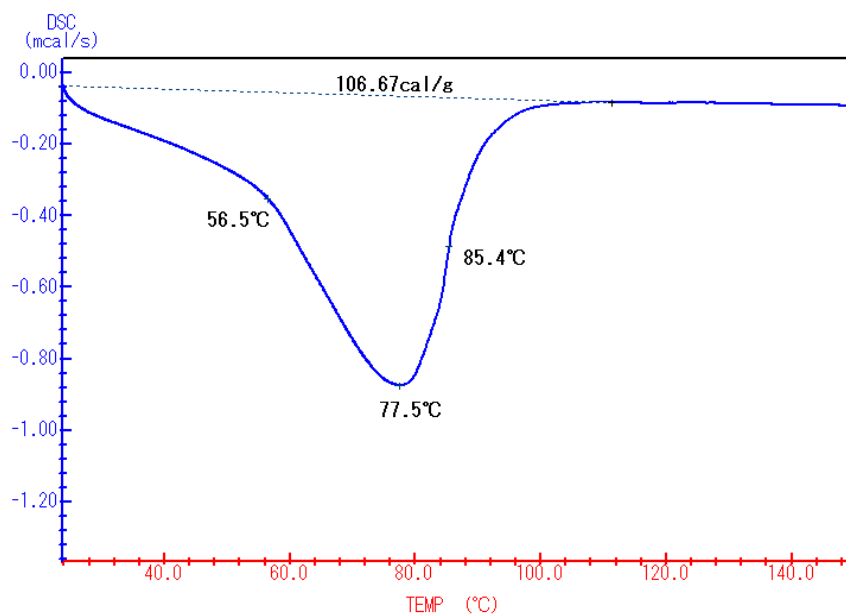


Fig. S13. DSC thermogram of $1\cdot\text{HCl}\cdot 3\text{H}_2\text{O}$ showing the extrusion of the water molecules from the channel below 373 K.